Aggregated Electric Vehicle Load Modeling in Large-Scale Electric Power Systems

Bo Wang, *Student Member, IEEE*, Dongbo Zhao, *Senior Member, IEEE*, Payman Dehghanian, *Member, IEEE*, Yuting Tian, *Member, IEEE*, and Tianqi Hong, *Member, IEEE*

***Abstract*—Different electric vehicle (EV) charging algorithms result in different EV charging load profiles, that if aggregated, influence the power grid operation. The existing EV charging demand models are either based on the charging status upon EV arrival or smart charging algorithms reinforced with particular charging methods and/or charging levels. This article proposes a new data-driven approach for EV charging load modeling. We first introduce a mathematical model that characterizes the flexibility of EV charging demand. Advanced simulation procedures are then proposed to identify the parameters of different EV load models and simulate EV charging demand under different electricity market realizations. The proposed EV load modeling approach can simulate different EV operation schedules, charging levels, and customer participation as a benchmark system. The proposed framework will also provide informative guidelines to transmission system operators for EV charging infrastructure planning in modern power systems.**

***Index Terms*—Electric vehicle (EV), EV charging methods, joint optimization, load flexibility, load modeling.**

NOMENCLATURE

Indices

i	Index for generating units (1,...,n).
k	Index for time steps (1,...,K).

Parameters

α	Ratio of regulation capacity to regulation limits.
α_c, α_d	Charge/discharge efficiency of the battery.
β	Ratio of regulation capacity that storage units can provide to the total regulation capacity needed in the system.
γ	Penalty factor for deviations from daily consumption of the PEVs.
ρ	Ratio of spinning reserve to load demand.
Δt	Length of the time step.
Λ_R	Total power output of renewables.
ς	Maximum flexibility of PEV loads.
c_d	Battery degradation cost per MWh.
E_C	Forecasted energy consumption of EVCSs in the next 24 h.
E_s	Energy consumption of EVs by swapping the batteries.
$f_c^{\max}$	Maximum frequency regulation capacity needed in the system.
L_F	Electricity demand for EV fast charging.
L_O	Original customer electricity demand.
V_C	Value of renewable energy curtailment.
V_F	Value of frequency regulation provided by the storage units.
V_S	Value of PHEV load shedding (i.e., gas price).

Variables

$\Delta P_{G,i}$	Ramp rate of generating unit i.
B_s	Energy stored in battery swapping station.
$C_i(P_{G,i})$	Operating cost function of generating unit i.
f_c	Frequency regulation capacity of the aggregated EV load demand.
f_l	Frequency regulation limit of the aggregated EV load demand.
L_c	Total energy allocated to EVCSs.
P_C	Curtailed power of renewables.
P_G	Active power of generating units.
P_{net}	Vector of the net generation.
P_R	Effective active power of renewables integrated into the power grid.
$R_{G,i}$	Reserve of power generating unit i.
u_c	Supplied power from the grid to BSS.
u_d	Delivered power from BSS to the grid.
u_l	Charging power to EVCSs.
u_{ls}	PHEV load shed by EVCS but met by the gas station.

Manuscript received November 3, 2019; revised January 17, 2020 and March 8, 2020; accepted April 10, 2020. Date of publication April 16, 2020; date of current version September 18, 2020. Paper 2019-AAAE-1316.R2, approved for publication in the IEEE TRANSACTION ON INDUSTRY APPLICATIONS by Energy Systems Committee of the IEEE Industry Application Society. This work was supported in part by the U.S. Department of Energy Office of Electricity under the Advanced Grid Modeling Program. *(Corresponding author: Payman Dehghanian)*

Bo Wang and Payman Dehghanian are with the Department of Electrical and Computer Engineering, The George Washington University, Washington, DC 20052 USA (e-mail: wangbo@gwu.edu; payman@gwu.edu).

Dongbo Zhao, Yuting Tian, and Tianqi Hong are with the Energy Systems Division, Argonne National Laboratory, Argonne, IL 60439 USA (e-mail: dongbo.zhao@anl.gov; ytian@anl.gov; thong@anl.gov).

Color versions of one or more of the figures in this article are available online at https://ieeexplore.ieee.org.

Digital Object Identifier 10.1109/TIA.2020.2988019

I. INTRODUCTION

ELECTRIC VEHICLES (EVs) bring about unique features and promising advantages in our modern society; just to name a few, they reduce the use of unsustainable fossil fuels, mitigate the greenhouse emissions from transportation sector, and improve the energy conversion efficiency compared to the combustion vehicles. Lithium-ion batteries are typically

employed as the power source for EVs. Constant current constant voltage (CC-CV) and constant power constant voltage (CP-CV) charging mechanisms are frequently employed to charge the EV batteries. Both charging strategies characterize a linear stage of charge (SOC) profile until about 95% of the battery is charged [1]. During the discharge process, the voltage would drop rapidly when the SOC is less than 5% (after roughly 95% of the capacity is spent). From the EV aggregators' perspective, battery operation in the nonlinear SOC region, i.e., CV region during the charging period, cannot be included in the EV charging coordination schemes. Therefore, the SOC of the batteries is limited from 5% to 95% considering both battery operation and lifetime. In the common practice, several EV manufacturers recommend the SOC to be in the range of 20% to 90% considering the SOC impacts on the battery lifetime. Hence, charging load of a single EV is typically considered as a constant power load during the steady-state power grid operation [2].

The uncontrolled charging, which assumes EVs to begin charging immediately after arrival with continued charging until the battery is full or the next trip starts, may enforce EVs to charge during daytime with higher electricity prices. This, in turn, may increase the system peak load [3]. With the proliferation of EVs, the aggregated EV charging load imposes a significant impact on the power system load profile. The importance of EV load management has been recognized by the industry and different regulatory mechanisms have been proposed to manage the EV load. Currently, EV load models that the industry uses are based on the EV charging through rate design or demand response programs [4]. One approach to rate design for EVs is time-varying pricing, which includes time-of-use (TOU) and dynamic pricing. TOU is the simplest form of time-varying pricing and has been widely used in the utilities. It features low communication requirements and is easy to be applied in practice. However, the TOU rates can change the charging behavior and may result in spikes in the load curve as EV customers may simultaneously charge their EVs during the lowest price period. Hence, this mechanism is suitable only when there is a very low EV penetration in the system. Dynamic pricing, which is another form of time-varying pricing, can be applied to scenarios with higher levels of EV penetration. However, it requires the PEV owners to be responsive to the price signals, while customers may not be conformable with its complexity. Demand response programs have been deployed to make EV charging load partially dispatchable. The EV load can be responsive to system needs with appropriate communication system. However, the partial control and decentralized scheduling of EVs is still unable to further optimize the EV charging schedules and the system objectives and performance requirements. Hence, the EV load models utilized in the industry are suitable for power grids with lower EV penetration and could not ensure robustness to the inherent uncertainties in customer behavior [5].

The international renewable energy agency published a road map to year 2050 about the global energy transformation. This report makes clear that an energy transition is urgently required, and that renewable energy, energy efficiency, and electrification are the three cornerstones of this transition [6]. In order to limit the rise in global temperature to well below 2 °C above the preindustrial levels (based on the Paris agreement), electrification of heat and transport industries with renewable power is the key, together making up 60% of the emission mitigation potential [6]. The light-duty vehicles and heavy-duty vehicles together count for nearly 80% of the transport sector energy use in United States in 2018 [7]. Electrification of these vehicles will result in a structural change in the transport energy use. Although the current EV load models used by the industry are suitable only for low EV penetration levels, other commonly used load models in industry are outdated and cannot represent such emerging loads [8]. Additional research is needed to develop EV load modeling frameworks under higher penetration of EVs, capturing different charging mechanisms, and interactions between EV customers and the power grid.

Recently, the thermostatically controlled loads (TCLs) are adopted to provide frequency regulation to the system; the virtual battery models have been proposed in [9] as an accurate and simple model to capture the flexibility of the residential heating, ventilation, and air conditioning systems. The flexibility of the TCLs is defined as the set of permissible deviations from nominal power profile that result in temperature trajectories with respect to the units' dead-band constraints. The aggregate flexibility of the collection is the sum of the flexibility of the individual units, and hence, the priority-stack-based controller is used for TCLs in [10]. Flexibility metrics and characterization in power systems are extensively studied in [11]–[16]. With wide deployment of advanced metering infrastructure (AMI) in the distribution system [17] and direct load control implementation in the EV charging stations (EVCSs) [18], both the transient and steady-state characteristics of the aggregated EV loads are primarily driven by the EVCSs' control and operation strategies. A new EVCS architecture has been proposed in [19] that 1) follows the IEEE Std 1547-2018 and 2) is responsive to the frequency and voltage events during gird transient disturbances. During the power grid normal operations, the flexibility of the aggregated EV loads is much larger than that by the aggregated TCLs [20]. A centralized EV charging strategy has been proposed to manage the EV charging schedules and follow the wind and solar power generation [21]. EV fleets are also employed to provide frequency regulation in [22]. Therefore, the flexibility of the EV loads can also be harnessed during day-to-day normal operating conditions, particularly in systems with high penetration of variable renewable energies (VRE) such as wind and solar.

Power system operation flexibility is the system ability to respond to changes in demand and supply. VRE can increase the need for flexibility such as steeper ramps, deeper turn downs, and shorter peaks in system operations. As power systems evolve to incorporate more renewable energy and responsive demand, flexibility across all power system elements must be addressed by ensuring: flexible generation, flexible transmission, flexible demand-side resources, and flexible system operations [23]. The demand-side flexibility includes [24] 1) the daily load demand variation accounting for the shortage or surplus in renewable energies, 2) interday load dispatch to smoothen the load profile, 3) intrahour flexibility such as frequency regulation, etc. While the

flexibility of an energy storage unit [25] can be simply defined as the energy, power and ramp rate it provides, the flexibility of the aggregated EV load has to take into account many factors such as the EV customer behaviors, different charging methods and strategies. The EV loads using conductive charging—including level 1 and level 2 charging—can be regarded as the *deferrable loads* when the smart charging algorithms are employed. Based on the conductive charging principles, fast charging (FC) EV loads are assumed to be *inelastic* and the EV load should be charged once the EV is connected to the EV supply equipment (EVSE) [26]. The inductive charging, also called wireless charging, reveals similar load characteristics as conductive charging, and the load flexibility is mainly driven by the charging power rates. The battery swapping station (BSS) can swap the EV batteries with fresh batteries and the flexibility of EV load is further enhanced with the deployment of large BSSs. Detailed models for different charging methods and charging levels are discussed in [27]–[30]. However, research on the aggregated EV load modeling to analyze the impacts of different combinations of EV charging methods on the grid and the EV charging infrastructure expansion planning is found rare and missing in the literature.

In this article, this knowledge gap is filled by proposing a framework to model the aggregated EV load considering different EV charging mechanisms. With the steady-state time-varying characteristics of the aggregated EV load model, the system operators can have a better state estimation and energy management scheme to reduce the system operation cost. With the dynamic characteristics of the aggregated EV load model, the system operator can simulate and test the impacts of EVs and renewables on the system stability performance. With the multi-timescale flexibility that the aggregated EV load can provide, the system operators can avoid unnecessary expensive investments in the EV charging infrastructure (e.g., transformer upgrade) and alleviate the system flexibility enhancements needed to integrate higher penetration of VRE. The proposed model can also be used as a benchmark system to simulate the impacts of aggregated EV loads on the power grid. The main contributions of this article are summarized as follows.

1) The flexibility that the aggregated EV loads can provide is quantified and mathematical models are proposed to simulate the impacts of the aggregated EV loads on the power grid considering different communication scenarios (delays, etc.).
2) Simulation procedures are introduced to numerically identify the model parameters and provide guidelines for the system operators to integrate large numbers of EVs to the power grids of the future.

This article is organized as follows. Section II presents the suggested EV load models and associated flexibility metrics. Section III introduces the mathematical model formulated to consider different charging mechanisms and communication delay scenarios between EVs and the power system. The interactions between the EV charging loads and the power grid are then simulated through a two-stage energy management system (EMS), where the model parameter identification is accomplished through simulations. Section IV presents the numerical case studies and simulation results. Section V discusses several aspects of the proposed models, followed by the concluding remarks in Section VI.

II. Aggregated EV Load Modeling

Different EV charging methods and charging levels result in different load characteristics in the power grid. In this article and in order to accomplish the aggregated EV load modeling, several assumptions are made: 1) there exist sufficient number of EV charging infrastructure in the grid, and 2) the EV customer can select the charging mechanism based on his/her priorities and preferences. The supply and demand interactions in the market enforce the need for a certain level of adequacy in EV charging infrastructure. The plug-in EVs (PEVs) including battery EVs (BEVs) and plug-in hybrid EVs (PHEV) using conductive charging with level 1 and level 2 charging mechanisms are assumed to deploy smart charging algorithms; that is the energy demand of such EVs needs to be met upon EV departure. Furthermore, the PHEV load can be curtailed and gasoline can be used instead when necessary. The BSSs are assumed to have routine BEV customers who subscribe to the battery swapping services; also, the BEV customers who prefer to use the plug-in charging mode can still swap their batteries when the EV batteries are depleted and plug-in charging mode could not satisfy the next trip energy demand requirement. The BEV customers can alternatively use FC mechanisms. The aggregated EV load of the FC stations (FCSs) are assumed to be inelastic with no flexibility. Thus, the flexibility of aggregated EV load is largely driven by the EV load characteristic of the EVCSs and the BSSs.

A. Steady-State EV Load Characteristics

1) Aggregated EV Load Model of the EVCS: Many EV customers charge their EVs in the EVCS with level 1 and level 2 charging mechanisms. Let L_c denote the cumulative energy that is expected to be allocated to the PEVs in EVCSs; (1a) states that the $L_c(k+1)$ during the next time step $k+1$ is the sum of $L_c(k)$, the actual charging power u_l allocated to PEVs, and the power curtailed from the PHEVs but met by the gas stations u_{ls} at the current time step k. Equation (1b) restricts the PEV demand, and ς reflects the maximum flexibility of the PEV demand. u_l and u_{ls} are limited to the lower and upper bound capacities in (1c) and (1d), respectively,

$$L_c(k+1) = L_c(k) + \alpha_c \Delta t (u_l(k) + u_{ls}(k)) \quad \forall k \tag{1a}$$

$$0 \le L_c(k) \le (1+\varsigma) E_C \quad \forall k \tag{1b}$$

$$u_l^{min}(k) \le u_l(k) \le u_l^{\max}(k) \quad \forall k \tag{1c}$$

$$u_{ls}^{min}(k) \le u_{ls}(k) \le u_{ls}^{\max}(k) \quad \forall k. \tag{1d}$$

While E_C for the aggregated EVCSs can be predicted and is stable over a day, the charging power constraints are time dependent and are affected by the charging capacity, number of connected EVs, and charging algorithms. In this article, AMI is employed to enable the communication between the utilities and EVCSs. The control and coordination of EV charging by the EVCS is also activated. Therefore, the actual aggregated constraints

for EV charging can be calculated and provided to the system operator by EVCSs, and the charging power sent from the system operator to each EVCS can also be implemented through direct load control. The estimated aggregated constraints are based on the day-ahead forecast values. The difference between the estimation and actual implementation can be acquired via AMI and compensated periodically. It is assumed that the customers with PHEVs prefer to charge their vehicles in the EVCS, as the electricity cost is normally 2 or 3 times less than gas. However, when the cost of electricity is higher than that for the gas, e.g., during the peak hours of a year, both customers and the system operators are willing to let the PHEVs to fill the gas. The PHEV charging requests will be declined by the EVCS and the energy demand will be met by gas stations. So, the actual u_{ls} can be recorded by the smart meter. The estimated values of L_c and u_{ls} do not include the gas use for routine PHEV travels. Note that the aggregated EVCS model in (1) reflects the detailed models of EVCSs in [21]. As the charging algorithm for EVCSs in [21] is a centralized EV charging algorithm using direct load control, the optimization problem can be formulated in one stage, and the EV charging schedules can then be implemented to follow the calculated dispatch signals. The EVCS-level signals communication and control implementation have been tested by the EVCS in [18]. The utility-level communication and control have been demonstrated by a high-fidelity dynamic charging model in [28]. However, the online computation loop for the centralized EMS requires an established AMI in [17], which can communicate bidirectional signals every 5 min.

Based on (1), the aggregated EVCS load at each bus can be regarded as virtual batteries, where the battery energy of the PEV load increases gradually, and the charging constraints vary with time. When the uncontrolled charging strategy is employed, it will render little load flexibility to the grid. The EV load will be then modeled as inelastic load. This can be reflected in (1c) since the upper bound and lower bound charging constraints are equal. However, since it is assumed that there is sufficient number of charging infrastructure available in the system, there will be a large number of EVs connected to the grid as vehicles are not moving most of the time during a day. Some EVs only have a few miles of trip during a day and the EV can be charged even in the next day. The flexibility of individual EV loads is dependent on the daily driving miles and EV idle time. If the EV load is flexible and the required charging demand that needs to be met is longer than 24 h, it is defined as a *fully controllable* EV load. The EV load that can offer some flexibility in time, but has to be charged within 24 h, is defined as *deferrable* EV load. A few PEV load needs to be charged immediately once plugged-in as they are heavy-duty inelastic loads. With the proper charging priority and charging power schedules, a certain level of flexibility provided by the aggregated PEV loads could be maintained in the power grid. Some power system operating conditions that influence the daily total energy allocated to PEVs, e.g., during outages, would also affect the EV load flexibility. Fig. 1 shows the state transition of PEV loads in terms of system flexibility. It is worth mentioning that some of the customers may charge their EVs at private places not observable by the system operator. Hence, these EV loads could not be controlled and can be regarded as

Fig. 1. Transition of EV load flexibility.

inelastic loads. They can be aggregated to traditional loads and forecasted using load forecasting algorithms. Hence, the EVCS load model can still be effectively represented by (1) when the smart charging and private charging networks are not strongly coupled.

2) Aggregated EV Load Model of the BSS: Focusing on the BSSs, it can be regarded as a storage unit with fixed battery capacity but varying battery swapping demand during each time period. The energy stored in the BSS (B_s) and the charging and discharging power (u_c and u_d) should be within the corresponding limits. The battery swapping load can be regarded as an additive disturbance to the BSS. Note that E_s includes both the battery swapping load by the subscribed customer and the additive EV load by BEV customers who prefer plug-in charging but their charging demand cannot be met by using the plug-in charging mechanism

$$B_s(k+1) = B_s(k) + (\alpha_c u_c(k) - (\alpha_d)^{-1} u_d(k))\Delta t - E_s(k) \quad \forall k \tag{2a}$$

$$B_s^{\min} \le B_s(k) \le B_s^{\max} \quad \forall k \tag{2b}$$

$$0 \le u_c(k) \le u_c^{\max} \quad \forall k \tag{2c}$$

$$0 \le u_d(k) \le u_d^{\max} \quad \forall k. \tag{2d}$$

It is assumed that the vehicle to grid (V2G) function is enabled in the BSS. So, it can discharge the power to the grid acting as a storage unit. u_c and u_d are power variables observed in the grid side. The multiplication of the two variables is 0 so that the BSS does not charge and discharge simultaneously. However, this constraint is not included in (2). The convex problem (2) will yield the same results as the nonconvex problem with this constraint when the charging efficiency and battery degradation cost are considered. Note that the aggregated BSS model is based on the detailed model presented in [29] in which a single BSS is modeled as a queuing network: the EVs form an open queue and the batteries circulating in a closed queue. It is assumed that the BSS reserves enough number of fully-charged batteries for EVs to exchange as needed, there are enough number of swapping servers and the batteries can be swapped when the EVs arrive. So, the queuing network characteristic is maintained by the proposed aggregated model. The battery swapping load does not have a direct impact on the power flow balance, and the difference between the forecasted and actual battery swapping load can be considered in the next time interval by the EMS.

The aggregated BSS load at each bus can also be regarded as virtual batteries. Similar to regular batteries, the BSS has fixed energy and power capacity. Moreover, its flexibility is also affected by the battery swapping load. The BSSs typically reserve some fully-charged batteries for EVs to swap. When a large number of EVs need to swap the batteries, and at the same

time, the BSS has minimum number of batteries in reserve, the BSS will charge the batteries even during the peak load period to satisfy the demand, and the BSS is regarded as inelastic load. Otherwise, with enough energy and power capacity, the BSS can meet the daily battery swapping load economically and also increase or decrease the daily charging demand flexibly. Hence, Fig. 1 could also represent the state transitions of BSSs.

3) Aggregated EV Load Model of the FCS: Focusing on high power FCSs, the aggregated FC load is modeled as inelastic load and it can be forecasted directly using load forecasting algorithms. Gnann *et al.* [30] showed that the charging sessions for fast charging over the day follows a distribution where the charging sessions are mainly concentrated around the center of the day. The practical FCS operation data in [31] also indicates that the aggregated FC demand follows a certain curve and is predictable. Hence, the uncertainty of the FC EV load can be treated similar to that for traditional loads.

B. Dynamic EV Load Characteristics

EV loads can be regarded as constant power or constant current loads during the transient operating states; the dynamic behavior of the aggregated EV loads is, however, mainly decided by the EVCS controllers. If the EVCS design in [19] is used, both PEVs and BSSs can respond to system disturbances and try to ride-through during the system abnormal operating conditions automatically. Note that this is achieved through a decentralized architecture, where real-time communication between the EVSE and the EVCS or BSSs is available.

The dead band for the frequency response provided by the inverter-based loads is typically set as ± 0.2 Hz [19], [32], and the EV load can provide frequency regulation services during the system normal operating conditions. The automatic generation control (AGC) signals are sent from the system operator every 2 to 4 s, so the real-time communication between the EVCS and the utility is also required. The EVCS and BSS loads can respond to the frequency signals, e.g., the Reg$D$ signal from the Pennsylvania-New Jersey-Maryland Interconnection (PJM) market, where PJM is a regional transmission organization in the northeastern United States that coordinates the movement of wholesale electricity in all or parts of 13 states and the District of Columbia. The actual power for EVSEs is, hence, the sum of the dispatch and regulation power. As Reg$D$ signals are conditional neutrality signals, the EVCS can detect the actual EV SOC when the regulation signal is back to the neutrality; therefore, it will have little impacts on the dispatch during system normal operating conditions. The EVCSs and BSSs reveal a high performance in following the Reg$D$ signal, so the revenue achieved by providing this ancillary service is mainly dependent on the regulation capacity that the EV load could offer. Once the economic operation base point of the EVCS is decided by the economic dispatch optimization, the EVCS can follow the regulation signals based on the operation base point. The high and low regulation limits must fall within the EV charging and discharging power constraints, and the regulation limits are the sum of the PEV and BSS regulation bands as enforced in (3a). It is, here, assumed that the ratio of regulation capacity to the regulation limits is α. We also assume that the frequency regulation capacity needed for the system is $f_c^{\max}$ and the regulation up and down capacities are symmetric. The frequency regulation capacity ratio that all storage units can provide in the system is β. The actual frequency regulation capacity that the aggregated EV load can provide can be then represented in (3b)

$$\begin{aligned} f_l(k) = &\min(u_l(k) - u_l^{\min}, u_l^{\max} - u_l(k)) \\ &+ \min(u_c(k) - u_c^{\min}, u_c^{\max} - u_c(k)) \\ &+ \min(u_d(k) - u_d^{\min}, u_d^{\max} - u_d(k)) \qquad (3a) \\ f_c(k) = &\min(\alpha f_l(k), \beta f_c^{\max}). \qquad (3b) \end{aligned}$$

Note that the two dynamic characteristics can be realized simultaneously during grid transient state. If a frequency event occurs and the disturbance is higher than the predefined threshold, EVCSs and BSSs, which enable real-time communication only with EVSEs will activate the frequency-droop control to facilitate the grid to ride-through the disturbance. The EVCSs and BSSs, which enable real-time communication with EVSE and the utility will also follow the AGC signals and provide frequency regulation services.

C. Flexibility of the Aggregated EV Loads

We define the *day-ahead flexibility* of PEVs in EVCSs as the SOC range of the aggregated EVs and the daily EV load demand variation that do not affect the charging capabilities. If the PEVs are scheduled to prioritize the charging schedule based on both the departure time and the energy needed for charging, the individual PEVs can meet their charging demands and a certain level of flexibility can be maintained by the aggregated PEV load. While the PEV charging includes individual EV charging schedules, and the virtual battery model constraints are time-dependent, the BSSs are featured with fixed capacity and charging constraints. The flexibility of BSS is affected by the aggregated battery swapping load curve. The day-ahead flexibility can be, then, defined as the SOC range of the aggregated BSSs that has little impacts on the charging and discharging schedules and the battery swapping demand. Different from PEVs, the day-ahead flexibility of which needs to be obtained by simulations including individual PEVs, the day-ahead flexibility of BSSs can be explicitly obtained by the economic dispatch simulation, where the aggregated model can be used and it can be treated as a large battery storage.

The *intraday flexibility* of the aggregated EV load including different EV charging mechanisms can be defined as the ability to improve the system load factor. With a given daily charging demand of PEVs and a forecasted battery swapping curve of the BSSs, the EVCS, and BSS loads can be dispatched to meet the charging demand during the off-peak hours so as to minimize the load variations. This will result in significant improvements in the energy delivery efficiency and an increase in the system load factor. If the aggregated EV loads are assumed to participate in the ancillary service (AS) market and contribute to the frequency regulation, the *real-time flexibility* of the aggregated EV load can be then represented by f_c. Hence, we here limit the discussion of aggregated EV load models to system normal operating conditions.

III. Parameter Identification of the Aggregated EV Load Models

With the multitimescale flexibility that the aggregated EV loads can offer to the system, the flexibility of the EV loads can be quantified and utilized by the system operator during daily operations. As we, here, study the cases with significant EV penetration, the aggregated EV load will impact the market price; hence, a production cost modeling approach has to be implemented. The economic dispatch model is used in this article to take into account both dispatch and AS market (frequency regulation and spinning reserve), and the system daily normal operation is then studied.

A. Economic Dispatch Model for Parameter Identification

If the communication network latency is high and the AMI only supports the 5-min bidirectional communication, the aggregated EV load could not provide the frequency regulation services to the system. The proposed economic dispatch model for the system operator considering the EV load with different charging mechanisms is presented in (1), (2), and

$$\min \gamma(L_c(K+1)-E_C)^2+\sum_{k=1}^{K}(V_S u_{ls}(k)+V_C P_C(k)) + \sum_{k=1}^{K}\left(\sum_{i=1}^{n} C_i(P_{G,i}(k))+2c_d u_d(k)\right) \tag{4}$$

$$\sum_{i=1}^{n}(P_{R,i}(k)+P_{G,i}(k))+u_d(k)-u_c(k)-u_l(k) = L_O(k)+L_F(k) \qquad \forall k \tag{5}$$

$$P_{G,i}(k+1)=P_{G,i}(k)+\Delta P_{G,i}(k) \qquad \forall k\,\forall i \tag{6}$$

$$P_{G,i}^{\min} \le P_{G,i}(k) \le P_{G,i}^{\max} \qquad \forall k\,\forall i \tag{7}$$

$$\Delta P_{G,i}^{\min} \le \Delta P_{G,i}(k) \le \Delta P_{G,i}^{\max} \qquad \forall k\,\forall i \tag{8}$$

$$P_{C,i}(k)+P_{R,i}(k)=\Lambda_{R,i}(k) \qquad \forall k\,\forall i \tag{9}$$

$$0 \le P_{R,i}(k) \le \Lambda_{R,i}(k) \qquad \forall k\,\forall i \tag{10}$$

$$\boldsymbol{H}\cdot\boldsymbol{P}_{\mathbf{net}}(k) \le \boldsymbol{F} \qquad \forall k \tag{11}$$

where the objective function (4) minimizes the total dispatch cost by allocating both generation and EV loads. The objective function (4) consists of the penalty cost for the deviations from daily energy consumption of the PEVs, the shedding cost of PHEVs and the curtailment cost of renewable power, the quadratic generation cost of conventional generating units, and the cost for discharging EVs—the degradation cost of EVs is considered when the V2G operating mode results in extra battery cycles to EV customers. Equations (1) and (2) represent the state and input constraints of EVCS and BSS, respectively. Equation (5) enforces the power balance constraint. Equations (6)–(8) are the state equations for the conventional generating units. Equations (9) and (10) represent the intermittent renewable power output. Transmission line constraints are expressed in (11). F is the vector of the transmission line flow limits. $\boldsymbol{H}$ is the power transfer distribution factor matrix. $\boldsymbol{P}_{\mathbf{net}}$ is the vector storing intermediate calculation of the net generation at the network buses.

B. Co-Optimization of Energy and Ancillary Services

If the real-time communication between the EVCS and EVSEs is enabled, and EVCS and the utility can also interact in real-time, the aggregated EV loads can participate in the frequency regulation market. Compared with the sequential optimization in which energy and reserves were cleared sequentially, the co-optimization with a single dispatch solution for energy and AS market every five minutes results in a more optimal energy dispatch and AS reserve schedules. If $\mathrm{OF_{ED}}$ represents the objective function introduced in (4), the joint optimization model considering both energy dispatch and AS can be, then, represented by (1)–(3) and (5)–(14)

$$\min\ \mathrm{OF_{ED}}-\sum_{k=1}^{K}(V_F f_c(k)) \tag{12}$$

$$R_{G,i}(k) \le P_{G,i}^{\max}-P_{G,i}(k) \qquad \forall k\,\forall i \tag{13}$$

$$\sum_{i=1}^{n} R_{G,i}(k) \ge \rho L_O(k) \qquad \forall k \tag{14}$$

where the objective function (12) is to minimize the total dispatch cost minus the revenue of the frequency regulation provided by EVs. The regulation capacity provided by EVs is stated in (3). $R_{G,i}$ in (13) is the reserve provided by the online conventional generating unit i, ρ in (14) is the percentage of demand, which specifies the reserve requirement. Other equations are the same as those previously introduced in the economic dispatch model. Note that the joint optimization model in the PJM market is defined as a single dispatch solution for energy, regulation, synch reserves, and nonsynch reserves every five minutes [33]. We only model the energy dispatch and frequency regulation provided by the aggregated EV loads in the objective function to demonstrate the role of the aggregated EV load in the joint optimization. The benefits of the frequency regulation that EVs can provide are modeled as the negative cost to the system. In practice, other objective and constraints can be added to the co-optimization model, e.g., the frequency regulation provided by the conventional generating units [34].

C. Parameter Identification Procedure

The steps to simulate the EV charging load is illustrated in Fig. 2. The following procedure is proposed to simulate the EV charging loads.

1) Assuming a certain penetration level of BEVs, PHEVs, and EV charging infrastructure under a given market mechanism, the power grid operation data is imported by the regional independent system operator (ISO). Note that the market mechanism is driven by the customer demand and energy policy, and should include other information such as the EV and power sector expansion road maps.

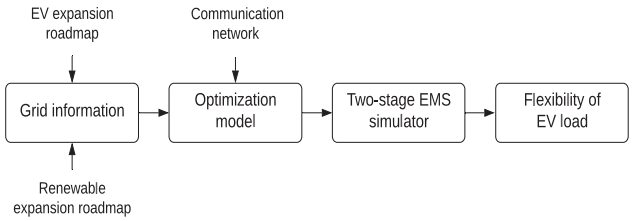

Fig. 2. Flowchart of the suggested parameter identification procedure.

2) Based on the market information, e.g., the type of ancillary service that the EV load provides, initial parameters for the proposed mathematical model are determined.
3) EV charging demand based on the proposed optimization model is simulated. The simulation is realized through a two-stage EMS architecture, where AMI is employed to achieve the communication between the system and EV customers.
4) Requisite parameters in the proposed mathematical model are calibrated through multiple simulations. As the simulator enables the interactions between the system operator and EV customers, both EV customer and power system objectives are considered.

The two-stage EMS utilized to identify the aggregated load model parameters either uses the economic dispatch model in Section III-A or the co-optimization model in Section III-B based on the communication delays and EV market participation. The EMS model is a modified version of the one presented in [21], and the entire simulation system is demonstrated in Fig. 3. Specifically, in Stage 1, as the BSS and PEV operation schedules are time dependent, the 24 h-ahead optimization problem is solved using the model predictive control in a receding-horizon manner, where the time step is set to 1 h, and the load, renewable, and EV load forecasts are updated hourly. The 3-h-ahead L_c and B_s are employed as the boundary conditions in Stage 2. In Stage 2, the same optimization problem is solved with a 3-h look-ahead time window, but the time step is 5 min and the look-ahead time window shrinks as time progresses until the next hour to recover back to 3 h. While the first stage includes the system-level forecasts and the 24-h-ahead optimization problem at each hour, the second stage uses short-time forecasts and the uploaded EV virtual battery model constraints to calculate the 5-min dispatch schedules. Furthermore, the second-stage EMS involves the interactions between the EVs and the ISOs. Bidirectional communications are achieved through the utility AMI. The priority of EV charging in EVCS has to meet the individual EV constraints; therefore, the EV information such as the SOC, departure time, and the minimum charging demand need to be collected from the connected EVs. The ISO receives the uploaded aggregated EV constraints, and at the same time, downloads the dispatch signals accordingly. So, the communication delay for the PEV dispatch is 5 min. AGC signals can also be sent to the BSSs and EVCSs, and are distributed proportionally if the real-time communication is enabled. The controller in BSSs and EVCSs can implement the integrated dispatch and AGC signals by using priority-stack-based control, which turns ON and turns OFF the EV load based on the charging priority or adjusting the duty cycle of the charging EVs proportionally. As FC EVs do not offer the flexibility to the system, only the aggregated load is forecasted and added to the associated bus during the parameter identification procedure.

IV. Numerical Case Studies

In this section, a test system is built to simulate the proposed aggregated EV load model. Then, the parameter identification procedure in Section III-C is applied to quantify the flexibility of the aggregated EV loads in the system.

A. Modified IEEE 118-Bus Test System With EV Loads

A modified IEEE 118-bus test system is utilized to simulate the aggregated EV load. As illustrated in Fig. 4, the system consists of 19 online conventional generating units. The test system specifications are taken from [35] with the following modifications: two wind farms with the total capacities of 500 MW and 750 MW are placed at bus 24 and bus 27, respectively. A photovoltaic (PV) power plant with a rated power of 650 MW is placed at bus 33. Hence, the total power capacity of the renewable sources is 1900 MW and features nearly 16% penetration in terms of the system generation capacity (23% penetration to the total online generation capacity). The predicted and actual data for renewables and load forecasts are taken from ERCOT and the weekly data captured in the week of December 18, 2017 in Texas is utilized in our simulations [36]. Scale factors of 1/16, 1/1.85, and 1/12.8 are applied for wind farms, PV plant, and the load, respectively. The day-ahead forecasts are replaced by the current-day forecasts in an hour-ahead manner. Both the renewable curtailment and PHEV shedding price are set to 40 \$/MWh. The spinning reserve requirement is set to 73 MW. α is assumed to be 0.7, and β is assumed to be 0.9 in the frequency regulation. $f_c^{\max}$ is set to 54.75 MW. The reserve and frequency regulation capacities are also scaled based on the ERCOT market [37].

The system is assumed to have 800 000 EVs accounting for 80% of the total vehicles. The charging and discharging efficiency is assumed 90%. The EV battery capacity (in linear SOC region) is 70 kWh and c_d is set to 21.4 \$/MWh. There are 100 000 EVs using FC, the aggregated FCS charging demand is modeled as an inelastic load at bus 112, and the forecasted load curve is derived from the distribution of daily FC loads in [26]. The actual energy consumption of the FC load is randomly generated using the Poisson probability distribution. There are 600 000 EVs using plug-in charging methods with the charging power of 10.2 kW, where 100 000 of them are PHEVs, and the aggregated EVCS load is placed at bus 115 as a virtual battery. The customers are assumed to plug-in their EVs to charge when the parking time is longer than half an hour and BEV customers will swap the depleted battery in BSS if the plug-in mode could not satisfy their next trip. Each aggregator is assumed to manage 100 to 200 connected EVs. Driving profiles for PEVs were obtained from the National Household Travel Survey 2017 database [38]. The estimated upper charging constraint is based on the availability of the aggregated EVs. The estimated total charging load is derived from the aggregated EV load demand. In total, 1000 driving profiles in Texas are randomly selected to account

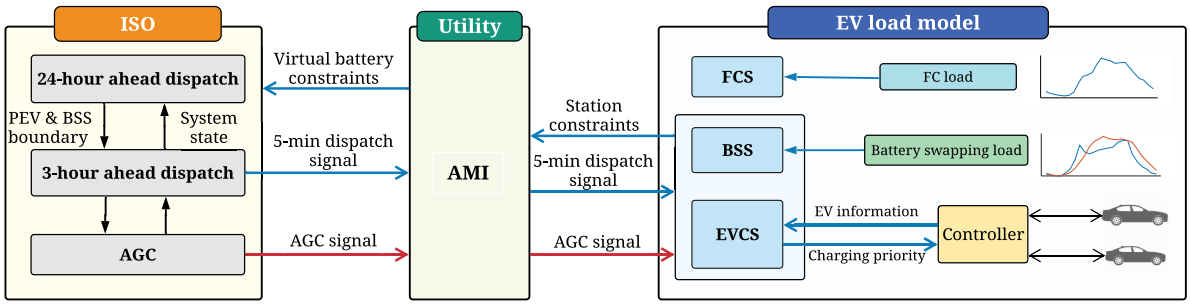

Fig. 3. Proposed framework to simulate the aggregated EV load models.

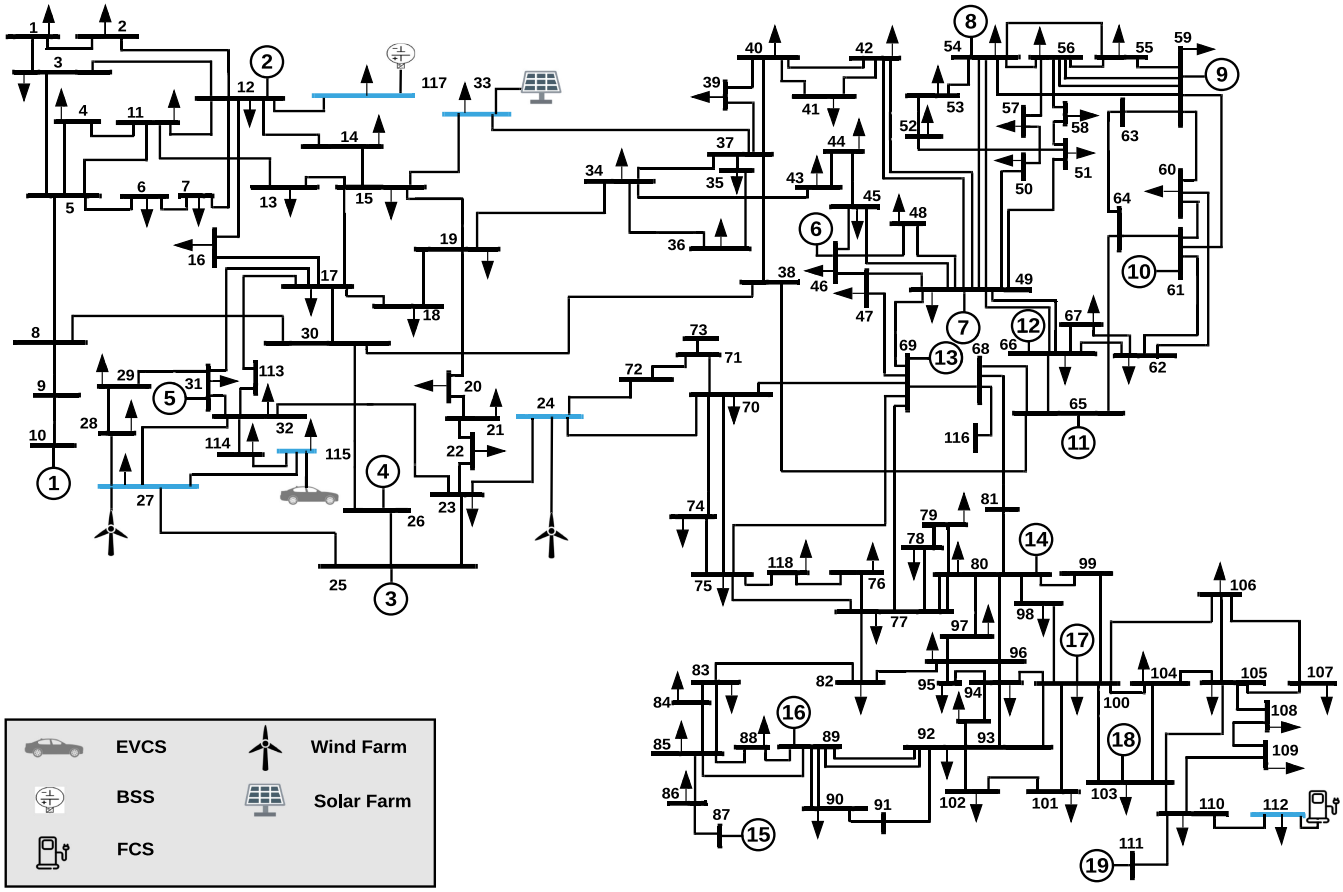

Fig. 4. Modified 118-bus test system with EV loads and renewables.

for the customer behaviors of the PEVs during the simulations. The initial SOC of the EVs is uniformly distributed between 0 to 80% of the battery capacity. The remaining 100 000 EVs are assumed to use battery swapping, the aggregated BSS is placed at bus 117, and the virtual battery capacity is set to 1050 MWh. The charge/discharge rate of the BSS is 242 MW. So, the BSS is able to be charged and discharged several cycles a day when necessary. We reserve 20% of the BSS capacity for battery swapping, and a penalty will be applied when the SOC of the BSS is lower than 20%. The SOC of the BSS could not be lower than 5%. The estimated energy consumption of battery swapping from customers who subscribe the service is derived from [39] based on the EV arrival rates. The actual battery swapping load from these customers is also generated using the Poisson probability distribution. The estimated energy consumption of PEV customers who use battery swapping services is assumed to be 0, and the actual battery swapping load from these customers is obtained from the simulations. Note that transmission line limits are not provided in the test system [35]. We assume that there is no congestion in transmission system, and hence, the EV loads are aggregated in one bus. When the congestion in the system needs to be considered, the EV loads need to be modeled in each bus. However, the optimization formulation will remain the same and the optimization model is still a convex problem.

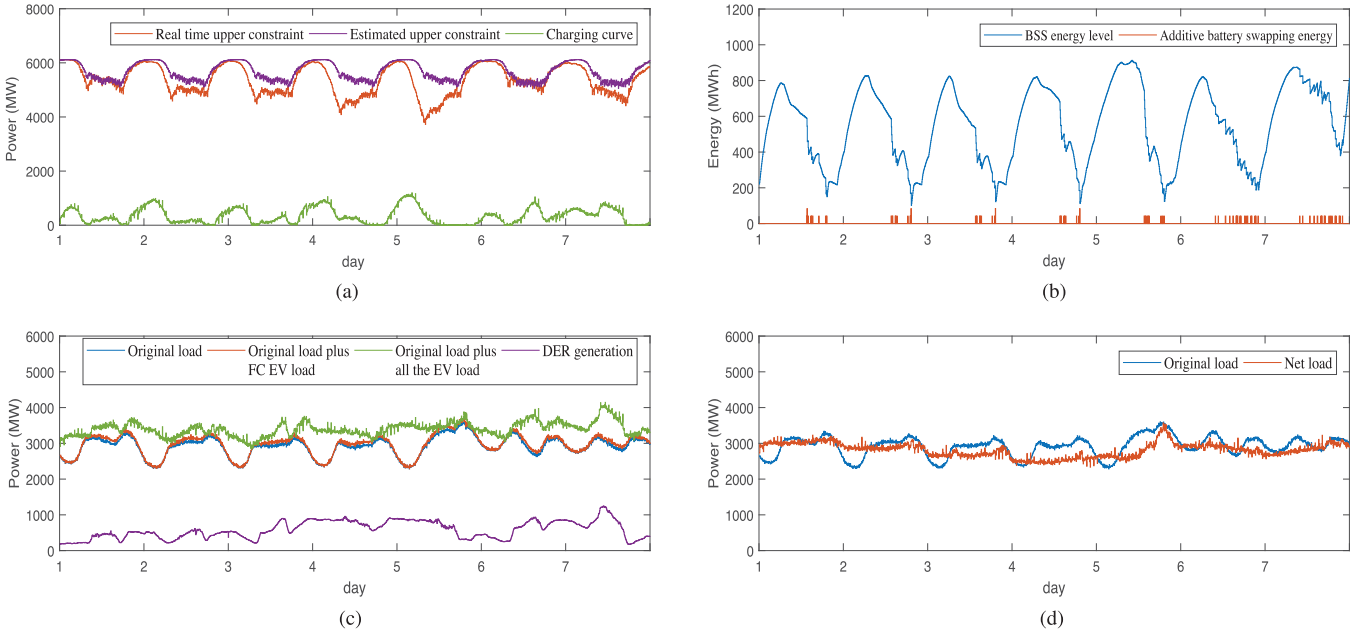

Fig. 5. Different aggregated EV loads and their impacts on the power system with 16% renewable penetration and 80% EV penetration. (a) EVCS charging curve. (b) BSS energy consumption. (c) EV load impact. (d) Net load.

B. Simulation Results

We run the seven-day economic dispatch simulations in the test system using the proposed framework. The CVX optimizer in MATLAB 2017a is employed to run all the test case scenarios. Fig. 5(a) shows that the real-time upper charging constraint of the aggregated EVCS charging is close to the estimated upper constraint (number of EVs parked), and the lower charging constraint is nearly 0, which is not included in the figure. The flexibility of the aggregated EVCS load is maintained during the week. The maximum charging power is less than 1200 MW and it is mainly decided by the economic dispatch outcome. Hence, a certain level of oversubscription in the EVCSs should be allowed. The aggregated BSS energy increases during the night and then decreases in the daytime [see Fig. 5(b)] because customers will mainly swap their batteries in the daytime. The additive battery swapping from PEV customers will decrease the energy of the aggregated BSS loads to less than 210 MWh (20% of the reserved BSS energy). The FC load shown in Fig. 5(c) will increase the peak of the original load. FC load only has a small ratio to the total EV load, and the extensive flexibility is provided by the EVCS and BSS loads. Hence, the aggregated EV load is not impacted a lot by the FC load; the total EV load including all the three charging methods shows a characteristic of renewable follower. The EMS reduces the daily variation of the peak and off-peak load in order to minimize the system total operation cost [see Fig. 5(d)], where the net load can also be represented by the total power output of the conventional generators. The total operation cost is found $ 12 527 577, and it is close to the lower bound of the optimal cost ($ 12 337 347). The lower bound is calculated using hourly data by assuming the perfect knowledge of load, FC and battery swapping curves. Also, the upper and lower charging constraints of aggregated EVCSs are relaxed to estimated values; the daily aggregated EVCS load is also assumed to be flexible that can be controlled during the calculation. Load factor for the week in this base case (TC1) scenario is 0.78 and the fuel cost of generators is 26.48 $/MWh on average, as shown in Table I.

TABLE I
COMPARISON OF THE LOAD FACTOR AND FUEL COST IN DIFFERENT CASES

Test Case	load factor	unit cost ($/MWh)
TC1	0.78	26.48
TC2	0.74	26.57
TC3	0.84	25.79

C. Parameter Identification Results for EV Flexibility

1) Day-Ahead Flexibility of the Aggregated EVCS and BSS Virtual Batteries: With the estimated energy consumption (E_C) of the EVs under plug-in mode for the next 24 h, the maximum and minimum charging demand do not significantly change during the week in the base case scenario. Fig. 6(a) and (b) illustrates that when the daily charging target is changed to 1.5 E_C, the maximum charging capacity will decrease sharply after the SOC of the EVCS virtual battery reaches 70%. When the daily charging target is changed to 0.5 E_C, the minimum charging capacity does not increase significantly. However, when the SOC of the virtual battery in Fig. 6(d) is below 30%, the battery swapping load from PEVs will increase dramatically as illustrated in Fig. 7. Therefore, it is suggested to maintain the SOC of EVCS virtual battery at least within 30% to 70% to maintain the flexibility of the PEV loads in the system. Keeping the range of SOC between 40% to 60% can ensure that the increase or decrease of 0.5 daily PEV demand will have little impacts on the charging constraints.

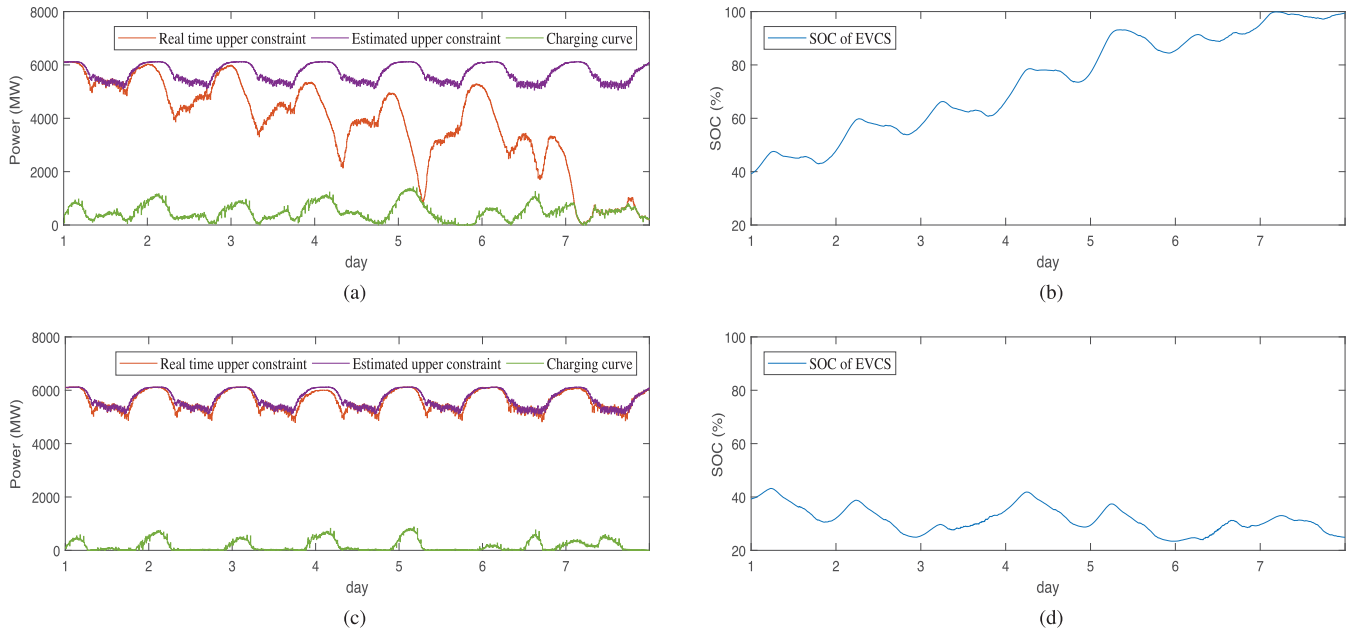

Fig. 6. Day-ahead flexibility of the aggregated PEV loads. (a) PEV charging curve with 1.5 E_C. (b) SOC of EVCS with 1.5 E_C. (c) PEV charging curve with 0.5 E_C. (d) SOC of EVCS with 0.5 E_C.

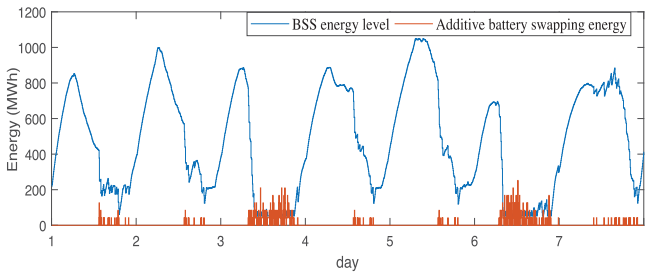

Fig. 7. Impact of additive BSS load from PEVs on the aggregated BSS virtual battery under 0.5 E_C.

While the charging constraints of EVCS virtual battery are time dependent, BSSs have a fixed number of batteries; hence, the charging and discharging power capacity of the aggregated BSS virtual battery will not be affected by the number of EVs under battery swapping mode in most cases. The flexibility of the BSS virtual battery can be evaluated by the economic dispatch optimization explicitly as storage units. Specifically, based on Fig. 5(b), the daily peak of the BSS is around 800 to 850 MWh except the fifth day with weekly peak reaching to 900 MWh. Hence, the fully controllable load is about 150 to 200 MWh and less than 100 MWh during the day with the weekly peak as the capacity of the BSS is 1050 MWh. Other parts are deferrable loads except that when the BSS reaches to the reserved capacity of 210 MWh. The BSS will charge from the grid to avoid the penalty of below 210 MWh, and the BSS load becomes inelastic when the stored energy in BSS is below 210 MWh.

2) Intraday Flexibility of the Aggregated EV Loads: The aggregated EV load in the base case scenario provides a large flexibility to the system, where the load factor is 0.78. If the EV penetration level changes to 20% of the total vehicles and the charging mechanism remains the same, the aggregated EV load will then mainly offer the valley filling during the off-peak hours [see Fig. 8(a)]. According to Fig. 8(b), although the net load decreases compared to that in the base case condition, the load factor decreases from 0.78 to 0.72. Hence, the lower the EV penetration, the lower the flexibility that the aggregated EV load can offer to the system. Under the same EV penetration and with the same number of battery swapping EVs compared to the base case condition, as the number of PEVs decreases to 200 000, then the number of FC EVs will increase to 500 000 that accounts for 50% of the vehicles. The FC load will increase the peak load significantly, and the EVCS and BSS virtual batteries will mainly achieve the valley filling so that there are no obvious super off-peak hours for EV charging [see Fig. 8(c)]. As shown in Table I, the load factor decreases to 0.74 and the average fuel cost of the system generators increases to 26.57 $/MWh in this case (TC2). It can also be seen from Fig. 8(d) that high penetration of FC EV loads will affect the flexibility of the aggregated EV load and may result in a higher peak of the net load compared to the original load. Note that this case is studied as the proposed model aims at simulating different EV charging levels and customer participation, and as neutral as possible to the technology types providing the charging services. In practice, if the home charging is not available to many customers and more FCSs have been built than the regular charging mechanisms in a region, there will be more FC EV load. However, the results indicate that the large FC EV load has negative impacts on the system, i.e., FCSs should not be the main charging method unless there are plenty of solar power to match the FC EV load and the flexibility needs are met by other energy resources in the grid.

3) Real-Time Flexibility of the Aggregated BSS and EVCS Virtual Batteries: With the real-time communication in the system and frequency regulation service provided by EV loads, the

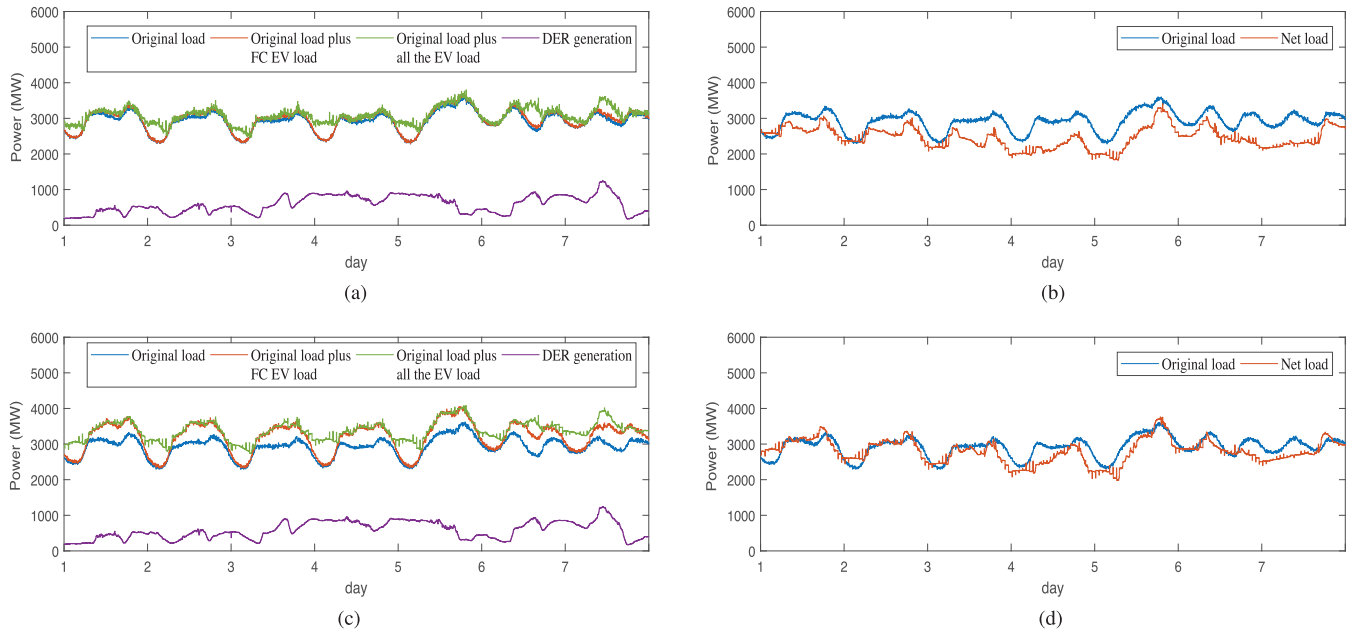

Fig. 8. Comparison of the intra-day flexibility for aggregated EV loads. (a) EV load impact with 20% EV penetration level. (b) Net load with 20% EV penetration level. (c) EV load impact with 50% FC EV. (d) Net load with 50% FC EV.

aggregated EV load can be simulated through the framework using the joint optimization model. We, here, employ the same simulation configuration in Section IV-B except that the joint optimization model is used instead of the economic dispatch model. With the first simulation conducted, the additive battery swapping load from PEVs can be achieved. If one replaces the estimated values (originally assumed as 0) with the simulation results obtained from the first simulation and run the simulation again, then the simulation results are demonstrated in Fig. 9. Compared to the economic dispatch model in the base case scenario, the EV charging schedules for EVCSs when the joint optimization model is applied are similar except for a few hours as shown in Fig. 9(a). This is because the frequency regulation capacity needed by the system is much smaller than the EV load needed to be dispatched. But the fuel cost decreases to 25.79 $/MWh because the joint optimization results in revenues on the frequency regulation provided by the aggregated EV loads. With better forecasts (considering the daily additive battery swapping load), Fig. 9(b) shows that the BSSs will also maintain their energy level higher than the reserved values and will avoid charging during peak hours to meet the EV demand of these customers. The load factor is then improved to 0.84 in this test case (TC3), as shown in Table I. Hence, the frequency regulation service provided by the EV loads can reduce the operation cost significantly, and only some EVCSs and BSSs with advanced design need to enable the real-time communication; this is because the needed frequency regulation capacity in such scenarios is much smaller than the load that needs to be dispatched. Also, if the additive battery swapping load is forecasted and considered by the ISO under high penetration of EVs, the system performance and its load factor will be improved. One needs to note that with better forecast results,

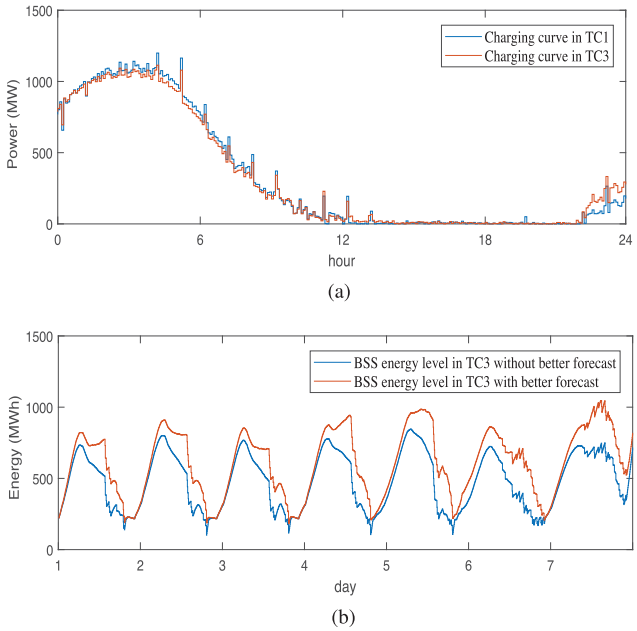

Fig. 9. Comparison between the economic dispatch model and the joint dispatch model. (a) PEV charging curve in the 5th day. (b) BSS energy consumption.

the stored energy in the BSS is mostly higher than the reserved energy; hence, there is no inelastic BSS load. However, as illustrated in Fig. 9(b), a better charging schedule of BSS is achieved at the cost of reducing the portion of fully controllable load that the BSS can provide. The intrinsic flexibility that the BSS provides to the system is the same, as it depends only on the physical constraints, e.g., BSS capacity and battery swapping profiles.

V. Discussions

As an initial work to characterize the flexibility of the aggregated EV load models in large-scale electric power system, this Section discusses the generality, precision, and applicability of the proposed model.

A. Parameter Calibrations and Generality of the Aggregated EV Load Model

While we simulated the aggregated EV load model in a modified IEEE 118-bus test system, the parameter identification procedure in Section III-C can be used to simulate aggregated EV load in any particular regions of interest, given that the data on the system typology, power gird operation, a certain penetration level of EVs, and different mixes of EV charging methods are available. FC and battery swapping loads can be generated or imported from the regional databases, the PEV customer behaviors can also be imported from local customer surveys as the proposed method is a data-driven approach. Simulation results in the base case condition can be followed by multiple simulations to quantify the flexibility of the aggregated EV loads. Thus, the proposed data-driven approach can be used as an effective tool for EV planning purposes at the system level to analyze the EV load impacts on the power grid. Note that in the case studies, it is assumed that whenever the EVs are parked for more than half an hour, the customers can connect their EVs to EVCSs. Most customers can swap their batteries immediately at the BSS, or charge their EVs via FCS whenever necessary. Hence, the proposed model can be universally used to simulate the aggregated EV load model when there are sufficient charging infrastructure, which means that enough number of charging infrastructure is available (charging capacity higher than forecasted EV load demand) to meet the customer charging demand and a certain level of infrastructure adequacy is maintained by the utility.

B. Impacts of Renewable Penetration Level on the Model Precision

In order to test the performance of the aggregated EV load under low renewable penetration level, the capacity of renewables is reduced from 1900 to 36 MW, while other parameters are kept the same as in the base case. The renewable capacity is then less than 0.6 % of the online generation capacity in the system and the impact of DERs on the system can be ignored as illustrated in Fig. 10(a). The EV load can reduce the daily variation of the peak and off-peak load effectively with the flexibility it can offer to the system, i.e., there are no load spikes compared with when the pricing-based EV load models are employed under high penetration of EVs. The net load in Fig. 10(b) is also similar as the original load plus the EV load in Fig. 10(a) as the DERs generation is small. Fig. 10(b) also indicates that the EV load will increase the total load and the net load profiles will not have obvious peak and off-peaks during most of the days in a week. The observation that the EV load contributes to a significant increase in the total load under high EV penetration levels is in line with the practical utility operation, e.g., 23% EV penetration

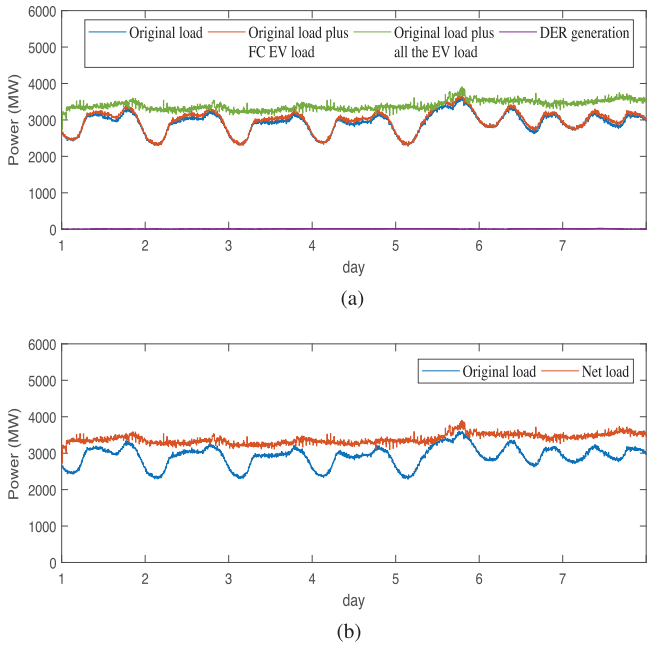

Fig. 10. Impact of aggregated EV loads on the power system with very low renewable penetration and 80% EV penetration. (a) EV load impact. (b) Net load.

in the California independent system operator market causes an obvious increase of the load [4]. Hence, the aggregated EV load models can effectively represent steady-state characteristics of aggregated EV load using smart charging.

The aggregated EV load can provide not only frequency regulation service but also load damping. New variable can be introduced to clearly model the frequency regulation, and the load damping that the aggregated EV load provides can be considered by modifying the joint optimization model. For instance, 270 MW EV load can be set to provide nearly 48 MW primary frequency response in the case studies. However, the ratio of the frequency regulation capacity to the frequency regulation limit, and the ratio of the load damping capacity to the load damping limit should be small so that the ancillary service provided by the aggregated EV load does not significantly impact the distribution system voltage and be less affected by the uncertainty in customer behaviors. It is also worth mentioning that under scenarios where VREs provide the main power and the system lacks large synchronous generators to maintain the grid stability, even the joint optimization model considering the abovementioned ancillary services provided by the EV load could not precisely characterize the grid flexibility requirements. Applying the proposed model to identify the aggregated EV load under such scenarios is oversimplification of the problem that may lead to significant errors.

C. Applicability of the Proposed EV Load Modeling Method

The proposed model is suitable to identify the aggregated EV load models for large-scale centralized power grids under higher EV penetration levels, in which the aggregated EV loads are predictable and the system dynamics do not vary sharply

within a short time interval. Hence, a large number of EVs are preferred, as the corresponding load is better predictable and less affected by the randomness of the customer behaviors based on the load aggregation effect. Also, the dispatch of the EV load could impact the market prices, and thus, a production cost modeling approach must be implemented [40]. The performance of the EMS will drop when the number of EVs is low, since the aggregated EV loads are less predictable in such circumstances. In contrast, the pricing-based EV charging strategies can be used when there are only a small number of EVs; these methods require little communication and the aggregated EV loads under these charging strategies do not have an obvious impact on the market prices. This is in line with practical system operation policies: large-scale storage units have to be modeled in the transmission system, while small storage units can follow the price signals and participate in energy arbitrage. It is also worth mentioning that the EV load can mitigate the impacts of the feeder-level interruptions and facilitate the feeder restoration process under interruptions. But the control and energy management schemes under these scenarios are not explored in this article. Hence, the proposed model could not fully characterize the reliability evaluation of the gird considering the EV loads.

VI. Conclusion

Virtual battery models for aggregated EVCSs with level 1 and level 2 charging mechanisms and aggregated BSSs are proposed in this article. A data-driven approach is also introduced to simulate the impacts of the aggregated EV loads on the system considering the two virtual battery models and FC EV loads. The proposed method can quantify the demand-side flexibility that the aggregated EV load can provide to the system. The proposed EV load modeling approach and associated test platform can also be used as a benchmark to simulate different EV penetration levels and market patterns and assess the impacts of different EV charging infrastructure expansion plans on the power grid operation.

Future research could be directed toward the following.

1) To study customer behaviors under the scenarios with insufficient EV charging infrastructure in the system and characterize how the flexibility of the aggregated EV load is affected by insufficient charging infrastructure.
2) Having plenty of EV charging infrastructure may be favorable to EV customers motivating many customers to switch from the combustion vehicles to EVs without the anxiety of EV travel distance. However, the simulation results indicate that the actual maximum charging power is mainly decided by the economic dispatch outcome. Moreover, maintaining a high adequacy of EV charging facilities may be costly to stakeholders and hard to pursue a timely investment return. Further research is needed to address the issue on how "sufficient" the EV charging infrastructure need to be to meet the customers charging demand, power system flexibility needs, and stakeholder's return on investment expectation. Regulatory mechanisms can be explored so that EVs can be charged based on the flexibility that individual EVs can provide.
3) The load damping provided by the demand side is fading fast as electronically controlled loads are taking over as the predominant component of the system loads [41]. The stakeholders and customers are also pursuing a target that the majority of the power supply come from VREs such as solar and wind [42]. Such trends impose significant challenges on the power grid frequency control. How the system operator can use the emerging loads such as the aggregated EVs and DERs to maintain the stability of the future inverter-based power systems and reformulate the joint dispatch model require both theoretical studies on the system stability (e.g., boundary conditions, frequency thresholds setting) and validations using hardware-in-loop simulations.
4) Detailed restoration strategies under interruption scenarios considering the EV loads should be studied. The system operator can also use the control and energy management schemes adaptively when different grid operating conditions unfold over time [43]. Then, the associated EV load models could be utilized for EV charging infrastructure expansion planning considering both reliability and economic evaluation [44], [45].
5) The proposed model studied the system-level EV charging impacts, while the regional numbers of EVs is stable and mobility of EVs does not significantly affect the power grid; the mobility and location of EVs are important factors for utility-level EV charging infrastructure planning. Coordination of transmission and distribution-level EV charging infrastructure expansion will result in more optimal decisions. Furthermore, the actual EV charging infrastructure expansion needs to consider other critical factors such as customer preferences, cost of different charging mechanisms, etc. The EV charging infrastructure expansion should consider the increasing rate of EV charging demand and all the above factors to achieve the dynamic equilibrium of the market.

References

[1] F. Marra, G. Y. Yang, C. Træholt, E. Larsen, C. N. Rasmussen, and S. You, "Demand profile study of battery electric vehicle under different charging options," in *Proc. IEEE Power Energy Soc. General Meeting*, Jul. 2012, pp. 1–7.

[2] A. Shukla, K. Verma, and R. Kumar, "Multi-stage voltage dependent load modelling of fast charging electric vehicle," in *Proc. 6th Int. Conf. Comput. Appl. Elect. Eng.-Recent Adv.*, Oct. 2017, pp. 86–91.

[3] M. Li *et al.*, "GIS-based probabilistic modeling of BEV charging load for australia," *IEEE Trans. Smart Grid*, vol. 10, no. 4, pp. 3525–3534, Jul. 2019.

[4] G. Fitzgerald, C. Nelder, and J. Newcomb. "Electric vehicles as distributed energy resources," Rocky Mountain Institute, Basalt, CO, USA, 2016. [Online]. Available: https://rmi.org/wp-content/uploads/2017/04/RMI_Electric_Vehicles_as_DER s_Final_V2.pdf

[5] D. S. Callaway and I. A. Hiskens, "Achieving controllability of electric loads," *Proc. IEEE*, vol. 99, no. 1, pp. 184–199, Jan. 2011.

[6] "Global energy transformation: A roadmap to 2050 (2019 edition)," Int. Renewable Energy Agency, Abu Dhabi, UAE, 2019. [Online]. Available: https://www.irena.org/publications/2019/Apr/Global-energy-transformatio n-A-roadmap-to-2050-2019Edition

[7] "Use of energy explained: Energy use for transportation," U.S. Energy Information Administration, Washington, DC, USA, 2018. [Online]. Available: https://www.eia.gov/energyexplained/use-of-energy/transportation-in-dep th.php

[8] A. Arif, Z. Wang, J. Wang, B. Mather, H. Bashualdo, and D. Zhao, "Load modeling—a review," *IEEE Trans. Smart Grid*, vol. 9, no. 6, pp. 5986–5999, Nov. 2018.

[9] J. T. Hughes, A. D. Domínguez-García, and K. Poolla, "Identification of virtual battery models for flexible loads," *IEEE Trans. Power Syst.*, vol. 31, no. 6, pp. 4660–4669, Nov. 2016.

[10] H. Hao, B. M. Sanandaji, K. Poolla, and T. L. Vincent, "Aggregate flexibility of thermostatically controlled loads," *IEEE Trans. Power Syst.*, vol. 30, no. 1, pp. 189–198, Jan. 2015.

[11] K. Oikonomou, M. Parvania, and R. Khatami, "Deliverable energy flexibility scheduling for active distribution networks," *IEEE Trans. Smart Grid*, vol. 11, no. 1, pp. 655–664, Jan. 2020.

[12] M. Khoshjahan, P. Dehghanian, M. Moeini-Aghtaie, and M. Fotuhi-Firuzabad, "Harnessing ramp capability of spinning reserve services for enhanced power grid flexibility," *IEEE Trans. Industry Appl.*, vol. 55, no. 6, pp. 7103–7112, Nov./Dec. 2019.

[13] B. Cui and X. A. Sun, "A new voltage stability-constrained optimal power-flow model: Sufficient condition, SOCP representation, and relaxation," *IEEE Trans. Power Syst.*, vol. 33, no. 5, pp. 5092–5102, Sep. 2018.

[14] F. Pourahmadi, H. Heidarabadi, S. H. Hosseini, and P. Dehghanian, "Dynamic uncertainty set characterization for bulk power grid flexibility assessment," *IEEE Syst. J.*, vol. 14, no. 1, pp. 718–728, Mar. 2020.

[15] J. Liu, S. Li, W. Zhang, J. L. Mathieu, and G. Rizzoni, "Planning and control of electric vehicles using dynamic energy capacity models," in *Proc. 52nd IEEE Conf. Decis. Control*, Dec. 2013, pp. 379–384.

[16] D. Hu and S. M. Ryan, "Stochastic vs. deterministic scheduling of a combined natural gas and power system with uncertain wind energy," *Int. J. Elect. Power Energy Syst.*, vol. 108, pp. 303–313, 2019.

[17] B. Wang, J. A. Camacho, G. M. Pulliam, A. H. Etemadi, and P. Dehghanian, "New reward and penalty scheme for electric distribution utilities employing load-based reliability indices," *IET Gener., Transmiss. Distribution*, vol. 12, no. 15, pp. 3647–3654, Aug. 2018.

[18] T. Bohn, C. Cortes, and H. Glenn, "Local automatic load control for electric vehicle smart charging systems extensible via OCPP using compact submeters," in *Proc. IEEE Transp. Electrific. Conf. Expo.*, Jun. 2017, pp. 724–731.

[19] B. Wang, P. Dehghanian, S. Wang, and M. Mitolo, "Electrical safety considerations in large-scale electric vehicle charging stations," *IEEE Trans. Industry Appl.*, vol. 55, no. 6, pp. 6603–6612, Nov./Dec. 2019.

[20] R. Garcia-Valle and J. A. P. Lopes, *Electric Vehicle Integration Into Modern Power Networks*. Berlin, Germany: Springer, 2012.

[21] B. Wang, P. Dehghanian, and D. Zhao, "Chance-constrained energy management system for power grids with high proliferation of renewables and electric vehicles," *IEEE Trans. Smart Grid*, vol. 11, no. 3, pp. 2324–2336, May 2020.

[22] G. Wenzel, M. Negrete-Pincetic, D. E. Olivares, J. MacDonald, and D. S. Callaway, "Real-time charging strategies for an electric vehicle aggregator to provide ancillary services," *IEEE Trans. Smart Grid*, vol. 9, no. 5, pp. 5141–5151, Sep. 2018.

[23] J. Cochran *et al.*, "Flexibility in 21st century power systems," to be published, doi: 10.2172/1130630.

[24] M. Rothleder and C. Loutan, "Chapter 6 - case study–renewable integration: Flexibility requirement, potential overgeneration, and frequency response challenges," in *Renewable Energy Integration*, 2nd ed., L. E.Jones, Ed. San Francisco, CA, USA: Academic, 2017, pp. 69–81.

[25] A. Ulbig and G. Andersson, "Analyzing operational flexibility of electric power systems," *Int. J. Elect. Power Energy Syst.*, vol. 72, pp. 155–164, 2015.

[26] R. Wolbertus and R. Van den Hoed, "Electric vehicle fast charging needs in cities and along corridors," *World Electric Vehicle J.*, vol. 10, no. 2, 2019, Art. no. 45.

[27] Z. Ding, Y. Lu, L. Zhang, W. Lee, and D. Chen, "A stochastic resource-planning scheme for PHEV charging station considering energy portfolio optimization and price-responsive demand," *IEEE Trans. Industry Appl.*, vol. 54, no. 6, pp. 5590–5598, Nov. 2018.

[28] Z. Yi *et al.*, "A highly efficient control framework for centralized residential charging coordination of large electric vehicle populations," *Int. J. Elect. Power Energy Syst.*, vol. 117, 2020, Art. no. 105661. [Online]. Available: http://www.sciencedirect.com/science/article/pii/S0142061519321775

[29] B. Sun, X. Tan, and D. H. K. Tsang, "Optimal charging operation of battery swapping and charging stations with qos guarantee," *IEEE Trans. Smart Grid*, vol. 9, no. 5, pp. 4689–4701, Sep. 2018.

[30] T. Gnann, S. Funke, N. Jakobsson, P. Plötz, F. Sprei, and A. Bennehag, "Fast charging infrastructure for electric vehicles: Today's situation and future needs," *Transp. Res. Part D, Transport Environ.*, vol. 62, pp. 314–329, 2018.

[31] Fastned, 2018. [Online]. Available: https://www.altenergymag.com/article/2018/07/why-fast-charging-stations -are-good-for-the-grid/29029

[32] U. Tamrakar, F. B. dos Reis, A. Luna, D. Shrestha, R. Fourney, and R. Tonkoski, "Virtual inertia emulation using commercial off-the-shelf inverters," in *Proc. IEEE Energy Convers. Congr. Expo.*, Sep. 2018, pp. 1111–1116.

[33] A. Giacomoni, K. Patel, and C. M. Velasco, "Price formation education 3: Reserves and co-optimization. PJM Interconnection." [Online]. Available: https://www.pjm.com/-/media/committees-groups/stakeholder-meetings/pric e-formation/20180117-am/20180117-price-formation-education-3-updated.ashx

[34] T. Ding, Z. Wu, J. Lv, Z. Bie, and X. Zhang, "Robust co-optimization to energy and ancillary service joint dispatch considering wind power uncertainties in real-time electricity markets," *IEEE Trans. Sustain. Energy*, vol. 7, no. 4, pp. 1547–1557, Oct. 2016.

[35] R. D. Zimmerman, C. E. Murillo-Sanchez, and R. J. Thomas, "Matpower: Steady-state operations, planning, and analysis tools for power systems research and education," *IEEE Trans. Power Syst.*, vol. 26, no. 1, pp. 12–19, Feb. 2011.

[36] ERCOT, 2018. [Online]. Available: http://www.ercot.com/gridinfo

[37] Future ancillary services in ERCOT, 2013. [Online]. Available: https://www.ferc.gov/CalendarFiles/20140421084800-ERCOT-ConceptPaper.pdf

[38] 2017 national household travel survey. U.S. Department of Transportation, Washington, DC, USA, [Online]. Available: https://nhts.ornl.gov

[39] L. Cheng, Y. Chang, J. Lin, and C. Singh, "Power system reliability assessment with electric vehicle integration using battery exchange mode," *IEEE Trans. Sustain. Energy*, vol. 4, no. 4, pp. 1034–1042, Oct. 2013.

[40] R. H. Byrne, R. J. Concepcion, and C. A. Silva-Monroy, "Estimating potential revenue from electrical energy storage in pjm," in *Proc. IEEE Power Energy Soc. General Meeting*, Jul. 2016, pp. 1–5.

[41] J. Undrill, "Primary frequency response and control of power system frequency," Lawrence Berkeley National Laboratory, Berkeley, CA, USA, 2018. [Online]. Available: https://www.ferc.gov/industries/electric/indus-act/reliability/frequenc y-control-requirements/primary-response.pdf

[42] M. Child, C. Kemfert, D. Bogdanov, and C. Breyer, "Flexible electricity generation, grid exchange and storage for the transition to a 100% renewable energy system in europe," *Renewable Energy*, vol. 139, pp. 80–101, 2019. [Online]. Available: http://www.sciencedirect.com/science/article/pii/S0960148119302319

[43] B. Wang, P. Dehghanian, D. Hu, S. Wang, and F. Wang, "Adaptive operation strategies for electric vehicle charging stations," in *Proc. IEEE Industry Appl. Soc. Annu. Meeting*, Sep. 2019, pp. 1–7.

[44] P. Zhou, R. Jin, and L. Fan, "Reliability and economic evaluation of power system with renewables: A review," *Renewable Sustain. Energy Rev.*, vol. 58, pp. 537–547, 2016. [Online]. Available: http://www.sciencedirect.com/science/article/pii/S136403211501727X

[45] T. Adefarati, R. Bansal, and J. J. Justo, "Reliability and economic evaluation of a microgrid power system," *Energy Procedia*, vol. 142, pp. 43–48, 2017. [Online]. Available: http://www.sciencedirect.com/science/article/pii/S1876610217357351

Bo Wang (Student Member, IEEE) received the B.Sc. degree in automation from Jilin University, Changchun, China, in 2013, and the M.Sc. degree in electrical power and energy from The George Washington University, Washington DC, USA, in 2015. He is currently working toward the Ph.D. degree with the Department of Electrical and Computer Engineering, The George Washington University, Washington, DC, USA.

His research interests include electric vehicles, power system optimization and control, and power system reliability.

Dongbo Zhao (Senior Member, IEEE) received the B.S. degree from Tsinghua University, Beijing, China, in 2008, the M.S. degree from Texas A&M University, College Station, TX, USA, in 2010, and the Ph.D. degree from the Georgia Institute of Technology, Atlanta, GA, USA, in 2015, all in electrical engineering.

He has worked with Eaton Corporation from 2014 to 2016 as a Lead Engineer in its Corporate Research and Technology Division, and with ABB in its US Corporate Research Center from 2010 to 2011. He is currently a Principal Energy System Scientist with Argonne National Laboratory, Lemont, IL, USA. He is also an Institute Fellow of Northwestern Argonne Institute of Science and Engineering of Northwestern University. His research interests include power system control, protection, reliability analysis, transmission and distribution automation, and electric market optimization.

Dr. Zhao is a member of IEEE Power and Energy Society, Industry Applications Society, and Industrial Electronics Society Societies. He is the Editor of IEEE TRANSACTIONS ON POWER DELIVERY, IEEE TRANSACTIONS ON SUSTAINABLE ENERGY, and IEEE Power Engineering Letters. He is the Subject Editor of subject, Power system operation and planning with renewable power generation of *IET Renewable Power Generation* and the Associate Editor for the IEEE ACCESS.

Payman Dehghanian (Member, IEEE) received the B.Sc. degree from the University of Tehran, Tehran, Iran, in 2009, the M.Sc. degree from the Sharif University of Technology, Tehran, Iran, in 2011, and the Ph.D. degree from Texas A&M University, College Station, TX, USA, in 2017, all in electrical engineering.

He is an Assistant Professor with the Department of Electrical and Computer Engineering, George Washington University, Washington, DC, USA. His research interests include power system protection and control, power system reliability and resiliency, asset management, and smart electricity grid applications.

Dr. Dehghanian is the recipient of the 2013 IEEE Iran Section Best M.Sc. Thesis Award in Electrical Engineering, the 2014 and 2015 IEEE Region 5 Outstanding Professional Achievement Awards, and the 2015 IEEE-HKN Outstanding Young Professional Award.

Yuting Tian (Member, IEEE) received the B.S. (Hons.) degree in electrical engineering from Sichuan University, Chengdu, China, in 2013, and the M.S. and Ph.D. degrees in electrical engineering from Michigan State University, East Lansing, MI, USA, in 2014 and 2018, respectively.

She is currently a Postdoctoral Appointee with the Energy Systems Division at Argonne National Laboratory, Lemont, IL, USA. Her research interests include power system modeling, energy storage systems, power system reliability, distributed energy resources, electricity market, and optimization applications.

Tianqi Hong (Member, IEEE) received the B.Sc. degree from Hohai University, Nanjing, China, in 2011, the M.Sc. degrees from the Southeast University, Nanjing, China and from the Engineering School of New York University, New York, NY, USA, in 2013, and the Ph.D. degree from New York University, New York, NY, USA, in 2016, all in electrical engineering.

He is currently a Postdoc Appointee with Argonne National Laboratory. Prior to this, he was a Postdoc Fellow with Engineering School of New York University in 2017. He was also a Senior Research Scientist with Unique Technical Services, LLC responsible for heavy-duty vehicle electrification, battery energy storage integration, and medium capacity microgrid. His main research interests include power system analysis, power electronics system, microgrid, and electromagnetic design.

Dr. Hong is also an active Reviewer for multiple international journals in the power engineering area.